Proceedings of the
44th IEEE Conference on Decision and Control, and
the European Control Conference 2005
Seville, Spain, December 12-15, 2005

Laboratory experimental testing of inerters

Christakis Papageorgiou and Malcolm C. Smith

Abstract— **This paper presents experimental results from the testing of mechanical networks involving inerter devices. The tests are carried out using a hydraulic ram actuator whose displacement is controlled in a closed-loop system. A methodology is proposed for the testing of inerter devices which amounts to the design of a buffer network to be connected in series with the inerter device during testing. This avoids instability and nonlinear phenomena which are otherwise observed with the testing of inertial loads using this type of hydraulic actuator. It is shown that the admittance of the inerter devices approaches the ideal inerter admittance over a useful frequency range.**

I. INTRODUCTION

Recently a new mechanical network element termed the "inerter" was introduced as an alternative to the mass element for *synthesis* of mechanical networks [1]. In the context of vehicle suspensions this was exploited in [2] by optimizing standard performance measures over low-order fixed-structure admittances and in [3] by optimizing the same performance measures over arbitrary positive real admittances using matrix inequalities. In both cases it was verified that the use of the inerter resulted in considerable improvement in ride comfort, handling and rejection of external loads. The inerter was also considered for the design of steering compensators for motorcycles [4]. It was shown that both the wobble and weave modes could be simultaneously stabilized which was otherwise impossible when using only a damper device.

The inerter is a mechanical two-terminal device with the property that the equal and opposite force applied at the two terminals is proportional to the *relative* acceleration between the terminals. Both terminals should be independently moveable. The inerter is in fact completely analogous to the capacitor, in the force-current analogy, whereas the mass element is analogous only to a grounded capacitor. The equation for the *ideal* inerter is given by,

$$F = b(\dot{v}_2 - \dot{v}_1) \tag{1}$$

where F is the force applied at the terminals, v_1, v_2 are the velocities of the terminals and b is a constant of proportionality called the inertance which has units of kilograms.

Various physical realizations of the ideal inerter have been described in [1] and [5]. Such a realization may be viewed as approximating its mathematical ideal in the same way that real springs, dampers, capacitors etc approximate their mathematical ideals. The two inerter devices whose testing is reported on here were manufactured in the Cambridge University Engineering Department (CUED) workshops. The first is a rack-and-pinion inerter and the second is a ballscrew inerter (Fig. 1). In both devices the required inertance is obtained by the rotation of a flywheel. In the first device the relative translation of the terminals is transduced into a rotation of the flywheel using a rack, pinion and gears while in the second device a ballscrew mechanism is used.

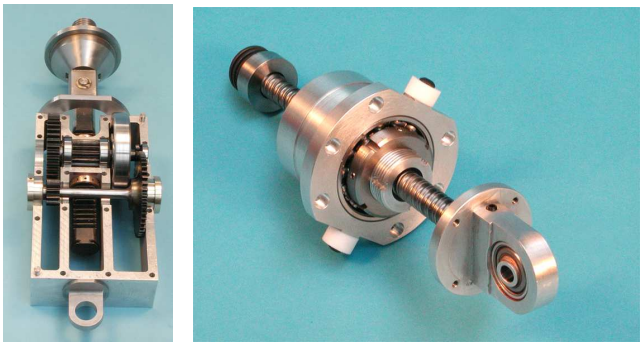

Fig. 1. Rack-and-pinion inerter (left) and ballscrew inerter (right) partially disassembled.

This paper considers the testing of these inerter devices in order to calculate their admittance functions and demonstrate the phase lead capability of mechanical networks involving such devices. This phase lead property cannot be obtained with spring-damper networks [1]. Also we wish to compare the characteristics of the devices with the characteristics of the ideal inerter and explain the causes of any deviations from theory. A more extended set of experimental results is given in [6].

II. THE HYDRAULIC TEST RIG

A Schenck hydraulic rig is used to test the inerter devices. The displacement of the hydraulic actuator is controlled in closed-loop with a PID controller and the inerter device or any other two-terminal mechanical network can be placed between the hydraulic actuator and a fixed point directly above it. The hydraulic rig works by regulating the oil flow in the chambers of a cylinder in order to move the piston (ram) according to the demands of the control system. The main elements of the hydraulic rig are the hydraulic power unit which provides a high pressure supply of oil, the servo-valve that regulates the flow of oil in the cylinder, the actuator by which we mean the ram, the control instrumentation and various sensors. The control instrumentation consists of a

This work was supported in part by EPSRC (U.K.) and RPF (Cyprus).

C. Papageorgiou is with the Department of Electrical and Computer Engineering of the University of Cyprus, Nicosia 1678, Cyprus, cpapageo@ucy.ac.cy

M. C. Smith is with the Control Group, Cambridge University Engineering Department, Cambridge CB2 1PZ, England, mcs@eng.cam.ac.uk

0-7803-9568-9/05/$20.00 ©2005 IEEE

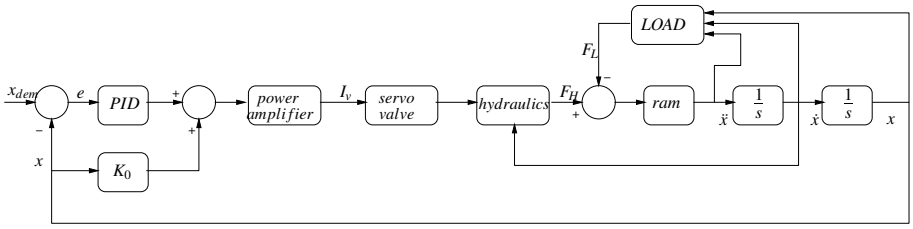

Fig. 2. Closed-loop system for the hydraulic test rig.

PID controller and a power amplifier that drives the servo-valve. The built-in controller [7] has various options including displacement control and force control. In this work we use the displacement control option. There are sensors which provide measurements of the ram displacement (x), the input current (I_v) to the servo-valve and the load force (F_L) on the mechanical specimen that is being tested. The measurements are filtered with analogue filters and logged using a data acquisition module. The demanded displacement (x_{dem}) is generated by a dSPACE processor interfacing with a Simulink application and is fed as an external input to the PID controller. Apart from the PID controller there is a proportional controller K_0 determined by a parameter in the range $[1,1023]$. Its purpose is to move the load to a desired position at the start of the testing procedure. During testing, the K_0 controller cannot be removed completely from the closed-loop system and although it does not receive the demanded displacement it receives as an input the actual displacement. The block diagram of the closed-loop system is shown in Fig. 2. The PID controller is determined by varying three parameters in the range $[1,999\times 16]$ which represent the proportional, derivative and integral terms but which cannot be related to a transfer function.

The hydraulic rig has been mainly used for testing damper loads for which the closed-loop system was stable. It was therefore important to anticipate the behaviour of the closed-loop system when testing loads of different dynamic characteristic in order to avoid any damage to the inerter devices and the rig. It was decided to test pure mass loads which have the same dynamic properties as the inerter devices (ignoring friction and backlash in the devices) and investigate closed-loop stability by identifying various transfer functions in the closed-loop system.

The real closed-loop system is quite complicated and nonlinear. Our objective is to identify its linear behaviour around an equilibrium point determined by the load condition and the initial ram displacement. For the identification we consider the closed-loop system of Fig. 3 where the open-loop transfer function $P(s)$ corresponds to the transfer function from the valve current I_v in amps to the measured ram displacement x in volts. The load characteristics are included in the transfer function $P(s)$. We will identify the closed-loop transfer functions from the demanded ram displacement x_{dem} to the ram displacement x and the valve current I_v which are called $T_0(s)$ and $T_1(s)$ respectively. When these are available we can calculate the plant transfer function as $P(s)=T_0(s)/T_1(s)$. Given the parallel structure of the controller, it is not possible to identify it with the available measurements. If $K_0=0$ then the product of the PID controller and the power amplifier could be identified as $K(s)H(s)=T_1(s)/(1-T_0(s))$.

The identification procedure involves the excitation of the demanded displacement with sinusoidal signals in an appropriate frequency range. At each frequency we calculate the phase and gain of the closed-loop transfer functions $T_0(s)$ and $T_1(s)$ using the correlation method [8, p.143]. The identification results are presented in the form of Bode diagrams of the relevant transfer functions.

III. Identification of the rig with mass loads

A. Testing with mass loads

The testing of the hydraulic rig was performed with two different controller settings which are named as K_1 ($P=529$, $K_0=1021$, $I=458$, $D=700$) and K_2 ($P=442$, $K_0=200$, $I=197$, $D=103$). As seen from the gains of the two controllers, the controller K_1 is a controller with 'larger' gain than controller K_2. The larger gain controller (K_1) was used to test two mass loads of 25 kg and 50 kg. It was also attempted to test a load of 75 kg but an instability occurred. The destabilizing effect of the increasing load mass on $T_0(s)$ is shown in Fig. 4. It is demonstrated by a lightly damped resonant peak at approximately 40 Hz and a sharp decrease in the phase. The effect of the increasing load mass on $sP(s)$ is shown in Fig. 5. It is demonstrated as an increase in the gain at high frequencies which is expected to cause stability problems unless the controller gain is appropriately reduced. The poor robustness of the K_1 controller led to the design of the K_2 controller which has smaller gains. The K_2 controller was able to stabilize the closed-loop system with mass loads up to 100 kg.

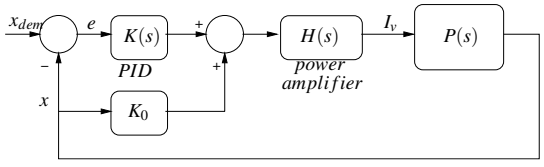

Fig. 3. Simple closed-loop system for the hydraulic test rig.

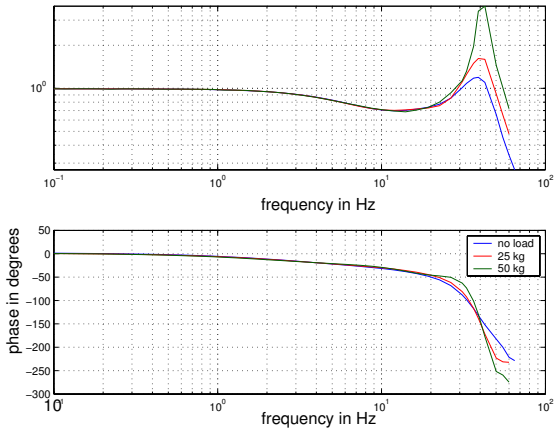

Fig. 4. $T_0(s)$ with controller K_1 for different mass loads.

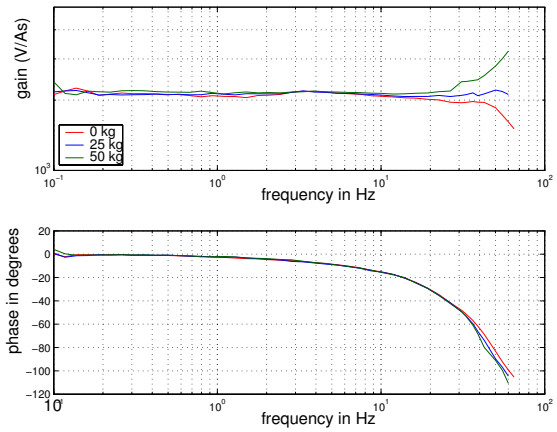

Fig. 5. Effect of the load mass on $sP(s)$ with controller K_1.

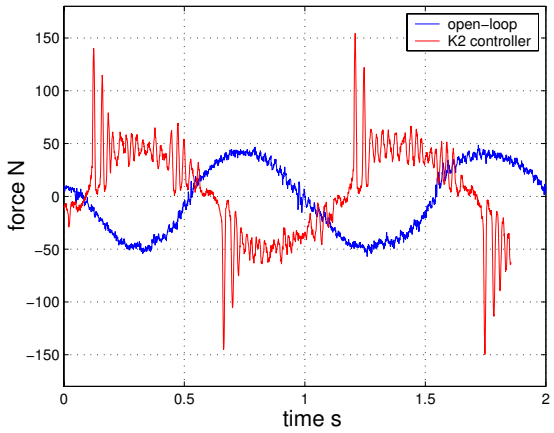

Fig. 6. The spiking characteristic in the force measurement.

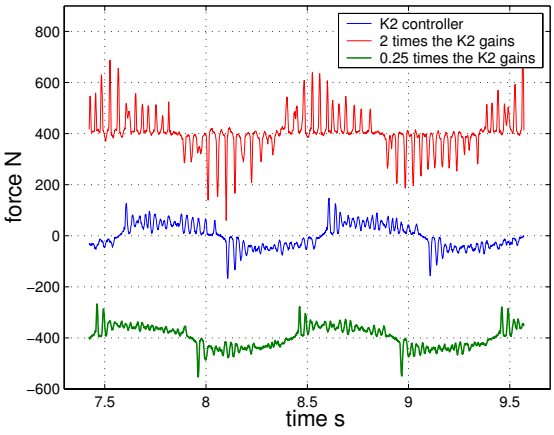

Fig. 7. The effect of the controller gain on the spiking characteristic.

IV. Testing of the Ballscrew Inerter

The robustness problem of a "large" gain controller with respect to increasing mass loads created a sense of caution for the first test of the ballscrew inerter. Thus the ballscrew inerter was tested with no flywheel (which implies minimum inertance) and with the more robust K_2 controller. The closed-loop system did not suffer from an instability but a different problem was identified related to the measurement of the load force. It was observed that the force signals were not sinusoidal due to a high-frequency, spiking characteristic which was superimposed on them. By conducting an open-loop test, which involved the sinusoidal displacement of the inerter by hand, it was verified that the spiking characteristic was a closed-loop phenomenon (See Fig. 6). This nonlinear characteristic was highly dependent on the controller gains as seen in Fig. 7, where the load force through the inerter is recorded for three different controllers for an excitation of 1 Hz. The inerter displacement in all three cases is approximately 10 mm p-p. The observation regarding the nonlinear behaviour of the closed-loop system is reinforced by a nonlinear instability observed in the force measurement when the inerter was excited at 2 Hz with the controller which has twice the gains of K_2 (See Fig. 8). Note that this instability was not observed at the excitation frequency of 1 Hz using the same controller gains.

V. Design of a Buffer Network

It was proposed to design a buffer to be placed in series with the inerter device during testing in order to remove the undesirable nonlinear characteristic in the force measurement. At this stage of the experiments it was difficult to give a precise diagnosis of the cause of the instability (due to the difficulty of identifying the dynamics of all elements in the loop exactly) but it was thought to be due to the dynamic characteristics of the inertial load combined with the backlash in the device. The strategy adopted was to design a buffer so that the total load seen by the hydraulic ram behaves as a damper load around the crossover frequency of the closed-loop system. The proposed buffer is a parallel combination of a spring and a damper (See Fig. 9). The admittance of the network is given by,

$$Y(s) = \frac{\hat{F}}{\hat{d}} = bs\left(\frac{k/b}{s^2+(c/b)s+k/b}\right)(1+(c/k)s).$$

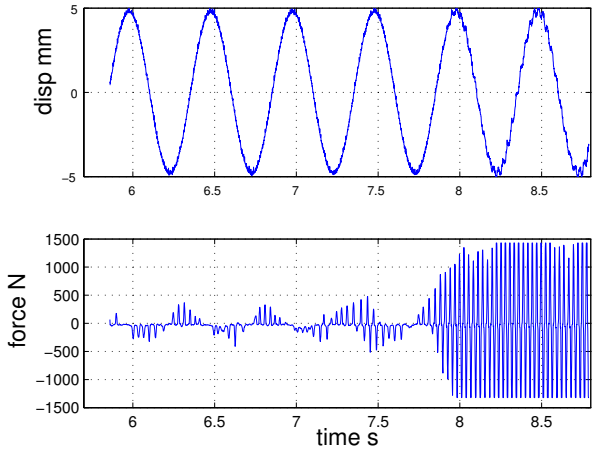

Fig. 8. Nonlinear instability when testing the ballscrew inerter.

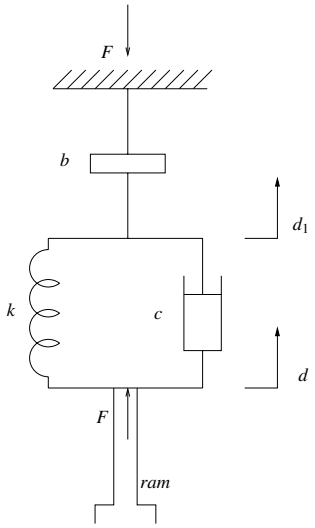

Fig. 9. Mechanical network for testing inerter devices.

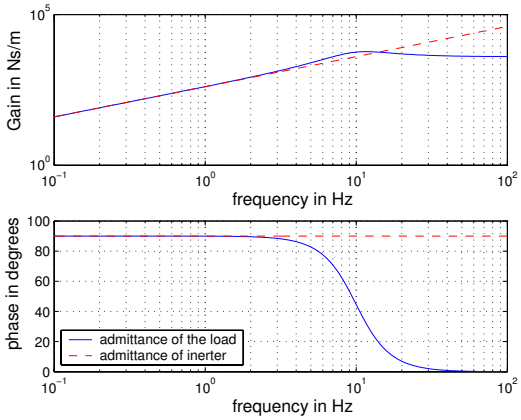

Fig. 10. Theoretical comparison of the load admittance with the inerter admittance.

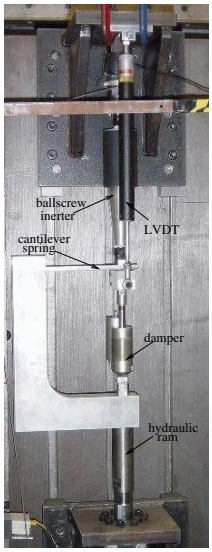

Fig. 11. The mechanical network on the hydraulic test rig.

The load behaves as an inerter (bs) at low frequencies and as a damper (c) at high frequencies as shown in Fig. 10 using the values $k = 253$ kN/m, $c = 4$ kNs/m and $b = 64$ kg. Such a network was designed and built at CUED and was placed on the hydraulic test rig as shown in Fig. 11. A displacement sensor (LVDT) is placed across the inerter so that a calculation of the inerter admittance is possible. The spring effect is produced through the use of a titanium spring cantilever which is supported by an L-shaped aluminium frame. The spring rate was calculated as 250 kN/m and the damper rate was approximately 4 kNs/m.

VI. Testing of Inerter Devices with the Buffer Network

A. Force measurements with the ballscrew inerter

The buffer was successful in removing the spiking characteristic in the force measurements. This is shown in Fig. 12 where a comparison is presented with the force signals obtained when the inerter (no flywheel) was tested on its own at frequencies of 4, 11 and 20 Hz.

B. Admittance of the ballscrew inerter

The admittance is the transfer function from the relative velocity of the inerter terminals to the force through the inerter, which are both internal signals of the closed-loop system. The admittance is calculated by dividing the identified closed-loop transfer functions from the demanded displacement to the pre-mentioned internal signals. The identification procedure was applied when the ballscrew inerter had no flywheel, an intermediate flywheel and a large flywheel. The frequency range was given by $[0.1, 30]$ Hz and it was spanned by 30 logarithmically spaced points. The admittances are presented in Fig. 13. The ideal inerter admittance is almost achieved in an intermediate frequency range in all three cases. In this frequency range the phase is advancing towards 80^o while the gain is rising at 20 dB/dec. The inertance of the device (shown on the plot) is estimated from the admittance functions by considering the 0 dB frequency crossing of the relevant part of the admittance. In the low frequency range

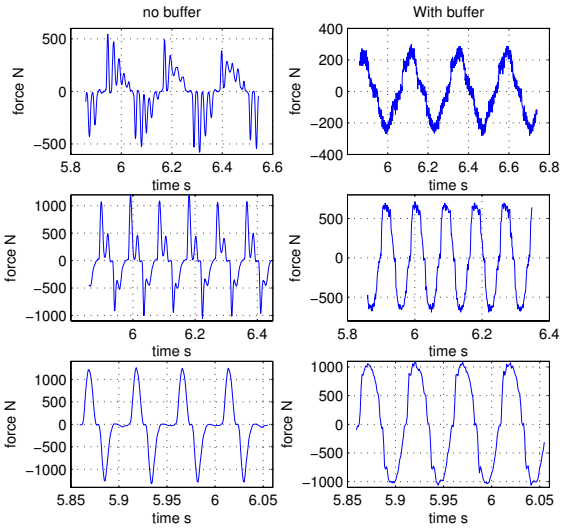

Fig. 12. Comparison of force signals recorded with and without the buffer.

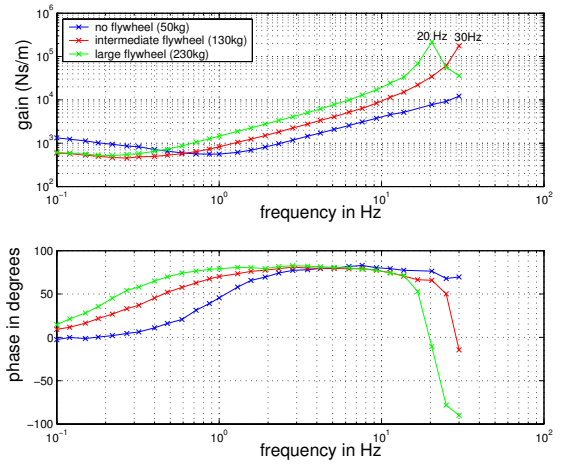

Fig. 13. The admittance of the ballscrew inerter with different flywheels.

the phase and gain information are inconsistent with linear theory since there is an increase in gain while the phase tends to zero. Such a characteristic can be explained by the dominant effect of friction. At high frequencies a resonance is observed in the device for the intermediate and the large flywheel. The peak in the gain is associated with a sharp decrease in the phase. The resonance is thought to be due to the compliance of the load cell which is used to measure the force. The load cell acts as a stiff spring in series with the inertance of the device with resonant frequency $\sqrt{(k_{\text{cell}}/b)}$.

The load admittance is calculated by considering the ram displacement and the force signal. The results for the three flywheel cases are shown in Fig. 14. Again the low frequency characteristics are dominated by friction. The effect of an increase in the inertance is to move the resonance of the load to a lower frequency and to make it less damped. The admittance of the load at high frequencies tends to the constant value of 4 kNs/m which agrees well with the shock absorber rate, and this is irrespective of the inertance value.

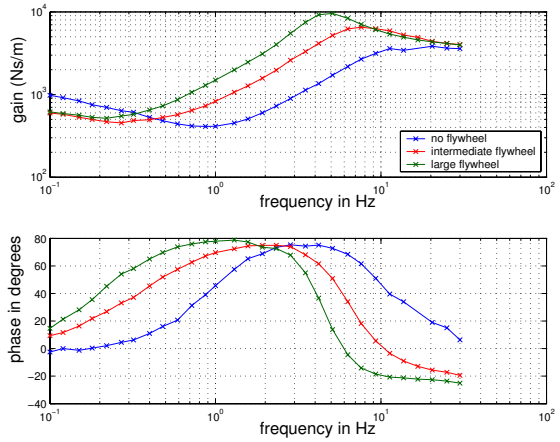

Fig. 14. The admittance of the load with the ballscrew inerter.

C. Force measurements with the rack-and-pinion inerter

As with the ballscrew inerter, the buffer is successful in removing the spiking characteristic observed in the force measurement when testing the rack-and-pinion inerter on its own. A comparison of some force measurements is presented in Fig. 15 for an excitation frequency of 1 and 5 Hz.

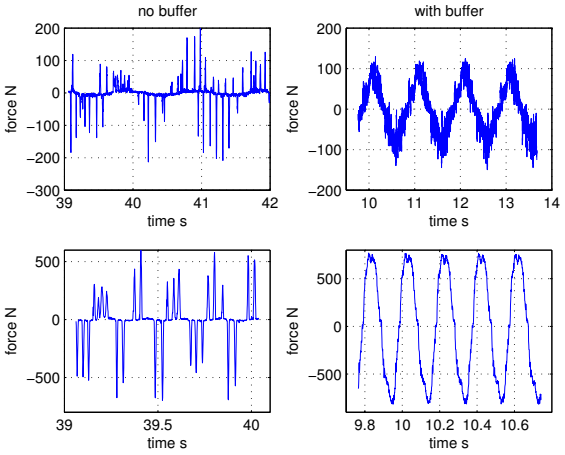

Fig. 15. Force measurements with and without the buffer for the rack-and-pinion inerter.

D. Admittance of the rack-and-pinion inerter

The rack-and-pinion inerter was tested in series with the buffer when the flywheel was removed and subsequently with an intermediate and a large flywheel. The calculation of the admittance was performed in a similar manner to that of the ballscrew inerter. The results are presented in Fig. 16 together with the estimated value of the inertance in each case. Note that with the large flywheel we reproduce the dynamic effect of over 700 kg mass with a device whose mass is ≈ 3.5 kg. As with the ballscrew inerter there exists an intermediate frequency range for which we obtain almost ideal inerter behaviour, i.e. a phase lead of approximately 80^o and a 20 dB/dec rise in the gain. The resonant peaks

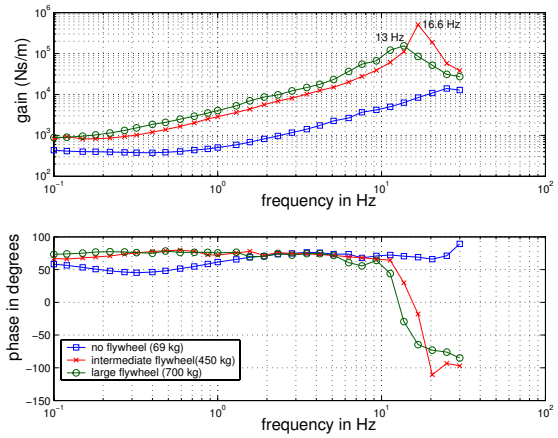

Fig. 16. The admittance of the rack-and-pinion inerter with different flywheels.

due to the load cell compliance appear at lower frequencies than with the ballscrew inerter due to the larger inertance values of the rack-and-pinion inerter.

The friction in the device dominates the low frequency range of the admittance function but its effect is different from that of the ballscrew inerter although it is again demonstrated as a discrepancy from linear theory (constant gain and a leading phase of $60^o - 70^o$). The difference of the friction in the two devices is investigated further by examining the force and displacement across the devices when excited at a frequency of 0.1 Hz. At this low frequency the inertial force is negligible and the measured force accounts mainly for the friction in the device. The force measurement is filtered further using an FIR filter. The results are shown in Fig. 17. In the case of the ballscrew inerter the force

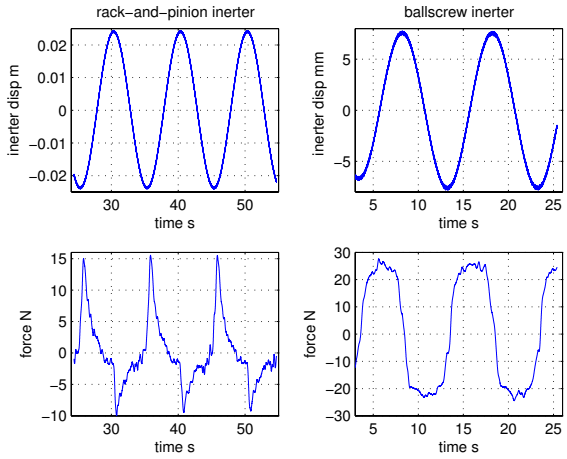

Fig. 17. Comparison of the friction effect in the two inerter devices.

measurement is almost a square wave of amplitude ≈ 25 N, implying a stiction effect which only changes direction when the velocity changes sign. In the case of the rack-and pinion inerter the force measurement has a triangular shape. The device experiences maximum friction when at its end-points and the magnitude of the friction is different at either end-point. Both behaviours are nonlinear and are the suggested cause for the discrepancies from linear theory in the bode diagrams of the admittance functions.

VII. Conclusions

Experiments were carried out to measure the mechanical admittance functions of two inerter devices built at Cambridge University Engineering Department (CUED). It was shown that the testing of the devices using a hydraulic damper test rig in displacement control mode can cause instability problems with increasing inertance unless the controller gains are reduced appropriately. It was shown that the the problem of the nonlinear spiking characteristic in the force measurement, which is observed when the inerter devices are tested on their own, can be removed by the design of a buffer network which is placed in series with the inerter device during testing. The buffer network makes the load appear as a damper around the crossover frequency of the closed-loop system. The admittance of the inerter devices approaches that of the ideal inerter in an intermediate frequency range but at low frequencies the behaviour of both devices is dominated by friction.

Acknowledgements and Notes

We are most grateful to Samuel Lesley, Neil Houghton, Peter Long, John Beavis, Barry Puddifoot and Alistair Ross for their work in the design and manufacture of the inerter prototypes. We would also like to thank David Cebon for making the Vehicle Dynamics Group's hydraulic ram available to us, and to Richard Roebuck for his assistance in the experiments.

References

[1] M. C. Smith. Synthesis of mechanical networks: The inerter. *IEEE Transactions on Automatic Control*, 47(10):1648–1662, 2002.

[2] M. C. Smith and F-C. Wang. Performance benefits in passive vehicle suspensions employing inerters. In *42nd IEEE Conference on Decision and Control*, pages 2258–2263, Hawaii, 2003.

[3] C. Papageorgiou and M.C. Smith. Positive real synthesis using matrix inequalities for mechanical networks: application to vehicle suspension. In *43rd IEEE Conference on Decision and Control*, pages 5455–5460, Bahamas, December 2004.

[4] S. Evangelou, D. J. N. Limebeer, R. S. Sharp, and M. C. Smith. Steering compensation for high-performance motorcycles. In *43rd IEEE Conference on Decision and Control*, Bahamas, 2004.

[5] M.C. Smith. Force-controlling mechanical device. patent pending, Intl. App. No. PCT/GB02/03056, priority date: 4 July 2001.

[6] C. Papageorgiou. Experimental testing of inerter devices. Technical report CUED/F-INFENG/TR.504, CUED, December 2004.

[7] CARL SCHENCK AG. *Adaptive Digital Controller RA311*. Issue 8.88.

[8] Lennart Ljung. *System identification:Theory for the user*. Prentice Hall, 1987.